Water-Glass-Based Composite Materials – Investigation into their Thermal Conductivity

R.A. Shishkin[*]

Ural Federal University, Yekaterinburg, Russian Federation

Abstract

Inorganic water-glass-based thermal pastes exhibit a higher thermal conductivity coefficient than silicon-based pastes. They can also be used at elevated temperatures. The dependence of thermal conductivity on filler content, curing agent, urea and hybrid fillers is studied. Special attention is paid to the curing chemistry of the thermal pastes during manufacturing. As a result, a number of composite materials with a significant improvement in thermal conductivity has been produced.

Keywords: Thermal paste, thermal conductivity, composite material, magnesium oxide, water glass

I. Introduction

Heat dissipation in LED installations limits any increase of the lighting power of installations with a constant number of diodes [1–3]. However, despite rather high thermal conductivity values of some silicon-based pastes (more than 4.0 W/m·K), the use of silver filler does not make them cost-effective for industrial application.

Commonly used silicon-based pastes have a thermal conductivity coefficient of no more than 1.0 W/m·K. Accordingly, a new composite material to intensify heat transfer between the LEDs and cooler is desirable. Several works deal with epoxy-matrix composites with enhanced thermal conductivity [4–9], however, such materials have a number of disadvantages, such as a narrow working temperature range, radiation decomposition, expensive fillers and low-thermal-conductive matrix. The only way to solve the problem of efficient heat dissipation is to study inorganic-matrix composite materials. Paper [10] pays special attention to the application of water-glass-based thermally conductive composite material as thermal grease. Magnesium-oxide-water glass compounds have a thermal conductivity coefficient (1.73 W/m·K) that is higher than that of silicon-based compounds. However, their enormous porosity (40–46 %) affects the thermal and mechanical properties, which could cause the composite material to suffer thermal stress during use.

Moreover, the above paper has emphasized the possibility of high-temperature application in thermal emission nuclear installations as grease between C-C refrigerator radiator plates and stainless steel heat pipes.

Further development is, in our opinion, mainly connected, with decreases in and modifications to the porosity of the composite materials with highly thermally conductive aids.

II. Experimental

The following reagents were used to obtain the samples: magnesium oxide (pure for analysis), water glass ("Stekolnoe proizvodstvo" Ltd., molar ratio SiO_2/Na_2O 3:1, density 1.42 g/sm³), sodium silicofluoride (pure for analysis), urea (pure for analysis) and graphite powder (Gl1 mark).

The components were weighed in Vibra HT-220 CE analytical scales (±0.0001 g), placed in a mortar and ground for 5–7 min. In a small crucible, the binder was weighed, the ground filler, curing agent and stabilizer were added, and then mixed to obtain a homogeneous mass with high viscosity. The mixture was tableted by filling it into cylindrical cells (diameter 10.0 mm, depth 3.5 mm) in a flat square fluoroplastic mold.

The samples were left in the air environment and at room temperature until the first step of drying and solidification was accomplished. The two processes occur simultaneously, but the duration varies for the different materials from a couple of hours to several days. The material can solidify or be in a half-hard tempered condition that is sufficient for further handling and processing.

The samples were removed from the mold and dried by heating at 150 °C for 1 h until evaporation of the volatile components was almost complete, and shrinkage and solidification were sufficiently complete in order to allow further heat treatment. The next technological step was to calcine the samples at a temperature of 650 °C without any prior aging.

The samples were mechanically processed to the dimensions required for analysis. The final samples with a weight of about 1 g in a tablet form were analyzed to determine the following properties:

• Bulk density (g/cm³)

$$\varrho = m/V \tag{1}$$

---

* Corresponding author: r.shishkin@yahoo.com

where m is the sample weight and V is the geometric volume;

- Water absorption in a vacuum (percent):

$$V = m_w \cdot 100/m_s \qquad (2)$$

where m_w is the weight of the absorbed water weight and m_s is the weight of the dried sample;

- Open porosity (percent):

$$P = m_w \cdot 100/V \qquad (3)$$

The tablets were weighed and the dimensions were measured with a thickness gauge (±0.01 mm). The samples were placed in distilled water and vacuum in a VDO3.5 "Templopribor" drying oven equipped with a 2NVR5DM pump (the ultimate residual pressure $6.6 \cdot 10^{-4}$ Pa). After 15 min holding for maximum water absorption, the samples were weighed. Eqs. (2) and (3) were used to calculate water absorption and porosity.

The results obtained are shown in Table 1.

The composite material samples were analyzed with Setsys Evolution equipment to study the optimal technological temperatures and physical-chemical processes during material hardening of the water-glass-based composite.

The heating rate was 3 °C/min and argon flow rate was 20 ml/min.

After being calcined at 650 °C, several samples were ground in a Retsch P100 planetary mill and the powder obtained underwent x-ray diffraction analysis conducted with a Shimadzu XRED-7000 x-ray diffractometer.

Thermal conductivity was measured according to the laser flash method with a NETZSCH LFA 457 MicroFlash at room temperature. Three samples in each parallel form for every set were measured seven times to increase measurement accuracy. The MicroFlash System measures thermal diffusivity and specific heat capacity and allows calculation of the thermal conductivity coefficient. The thermal conductivity is defined as $\lambda = (Q/A)/(DT/DL)$, where (Q/A) is the heat flux; Q is the amount of heat passing through a cross-section A of a sample; (DT/DL) is the resultant thermal gradient (where DT temperature difference; DL length along the heat flow).

The specific heat can be measured with the laser flash method by comparing the temperature changes of the investigated and a reference sample tested under the same conditions [11].

Table 1: Thermal conductivity and porosity evaluation of thermal grease samples (η – volume filling; P – open porosity; V – water absorption; ϱ – bulk density; P_θ – porosity change after calcination; V_θ – water absorption change; ϱ_θ – density change)

No	η	Thermal conductivity W/(m K)	Material properties after drying at 150 °C			Material properties after calcination at 650 °C					
			P	V	ϱ	P	P_θ	V	V_θ	ϱ	ϱ_θ
1	0.2	1.44±0.04	9.01	5.63	1.61	13.69	52	9.2	63	1.49	-7
2	0.25	1.48±0.04	19.21	10.93	1.76	20.92	9	12.97	19	1.61	-8
3	0.27	1.77±0.05	20.98	11.83	1.77	25.34	21	15.64	32	1.63	-8
4	0.28	1.68±0.05	22.61	12.04	1.87	26.42	17	15.42	28	1.71	-9
5	0.25	1.94±0.06	11.16	6.68	1.67	20.2	81	13.48	102	1.5	-1
6	0.25	2.03±0.06	6.87	4.05	1.71	18.18	165	11.74	190	1.55	-9
7	0.25	1.87±0.06	13.69	8.25	1.66	16.31	19	10.68	30	1.53	-8
8	0.25	1.87±0.06	14.24	8.81	1.75	18.27	21	10.32	15	1.61	-8
9	0.25	1.84±0.05	11.42	6.69	1.71	24.5	115	15.72	135	1.56	-9
10	0.25	1.71±0.05	19.12	12	1.59	25.96	36	17.96	49	1.44	-9
11	0.25	1.67±0.05	19.48	13.36	1.58	23.4	20	16.45	33	1.43	-10
12	0.25	2.27±0.07	12.21	7.41	1.65	15.53	27	10	35	1.55	-6
13	0.25	2.22±0.07	3.86	2.56	1.51	11.67	202	8.24	222	1.42	-6
14	0.25	2.00±0.06	4.43	3.03	1.54	17.5	278	12.16	301	1.45	-6
15	0.25	1.53±0.05	3.6	2.63	1.35	18.79	422	14.55	453	1.29	-5
16	0.25	1.59±0.05	17.28	13.26	1.3	23.4	35	19.12	44	1.22	-6
17	0.47	3.70±0.10	3.09	2.19	1.41	20.26	556	15.02	585	1.35	-4
18	0.35	3.09±0.09	7.45	4.69	1.57	15.6	110	10.4	122	1.5	-5

The thermal diffusivity α of a medium is the thermophysical property that determines the speed of heat propagation by conduction during changes of temperature over time. The higher the thermal diffusivity, the faster the heat propagation. Thermal diffusivity is related to thermal conductivity λ, specific heat C_p and density ϱ as follows:

$$\alpha = k/\varrho \cdot C_p \qquad (4)$$

The standard configuration was used with a $200-300$ ls pulse width.

III. Results and Discussion

Obviously, the application of a curing agent considerably affects the physicochemical curing processes in the composite material; it is therefore advisable to analyze the difference between water glass and magnesium oxide mixtures and the same mixtures with a curing agent.

At 137 °C a strongly pronounced endothermic effect (327.7 J/g) is observed, which is the result of water evaporation from the binder (Fig. 1). The total moisture loss is 26.98 %. At the further exothermal peak, the composite material is absolutely anhydrous. The exothermal effect (47.12 J/g) at 787 °C is conceivably due to crystallization of the amorphous silica contained in the water glass, which confirms the data in [12]. As the composite materials were prepared as described above, the thermal conductivity of samples containing amorphous silica was measured. No step-wise changes of thermal conductivity of composite materials with crystalline and amorphous silica were observed.

$Na_2Mg_5Si_{12}O_{30}$ and Na_2MgSiO_4 were calcination products.

The following studied sample was a mixture of water glass, magnesium oxide, and sodium fluorosilicate as a curing agent. Fig. 2 shows a thermogram of the sample.

The absorbed water evaporates at 133 °C with an endothermic effect 239.91 J/g. The total moisture loss is 25.68 %, that is evidently slightly different from the previous one. The sample was completely dehydrated by 700 °C. It should be mentioned that three major exothermal peaks in the thermogram are observed at 640 °C (21.62 J/g), 721 °C (17.16 J/g) and 890 °C (14.17 J/g). Two tiny minor peaks could be observed at 606 °C (0.65 J/g) and 820 °C (0.51 J/g).
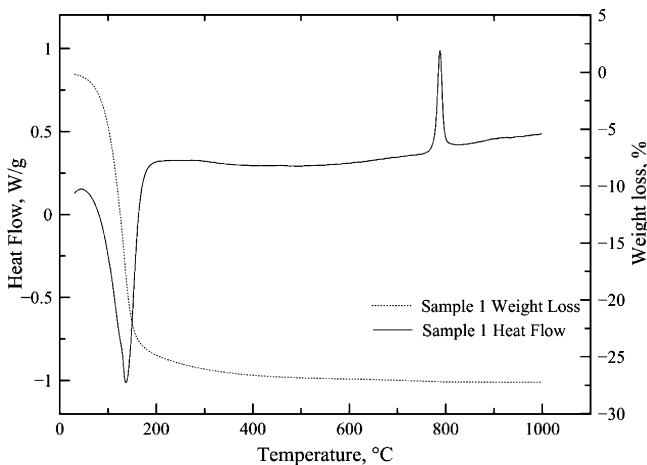

Fig. 1 : Thermal analysis of magnesium oxide and water glass mixture.
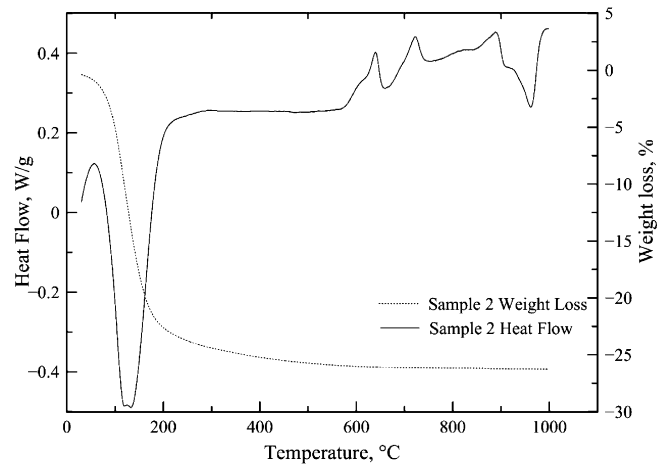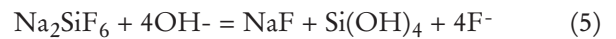

Fig. 2 : Thermal analysis of magnesium oxide, water glass and sodium fluorosilicate mixture.

These effects could be conceivably interpreted in the following way:

The sodium fluorosilicate reacts with the hydroxide at 606 °C:

$$Na_2SiF_6 + 4OH^- = NaF + Si(OH)_4 + 4F^- \qquad (5)$$

In turn, fluoride ions react with the alkali that is part of the water glass at 640 °C with a significant thermal effect, which is confirmed with thermodynamics calculations.

$$NaOH + F^- = NaF + OH^- \qquad (6)$$
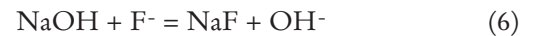
Amorphous silica crystallizes at lower temperatures (721 °C) owing to the chemical hardening.

Peaks at 820 and 890 °C can be accounted for by silica polymerization with the formation of complex silicates ($Na_2Mg_3Si_6O_{16}$, $Na_2Mg_5Si_{12}O_{30}$ and Na_2MgSiO_4)

The chemical reaction in the water glass system can be presented in the following way:

$$MgO + N_2SiO_3$$
$$\cdot 6H_2O \rightarrow Na_2Mg_5Si_{12}O_{30} \rightarrow Na_2MgSiO_4$$
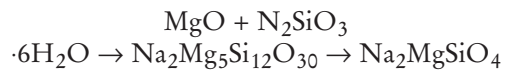
A significant endothermic effect is observed at 963 °C (27.79 J/g), which could be explained by the melting of the sodium fluoride (melting point 993 °C);

In the first set of the samples (1–4), the dependence of thermal conductivity on the magnesium oxide volume filling (20–28 vol%) with the addition of sodium fluorosilicate (15 wt% of binder weight) was studied. Obviously, a decrease in open porosity is observed in comparison with composite materials without a curing agent. Thus, the average porosity was about 20 %. It should be pointed out that the first sample has shown less porosity owing to lower viscosity during filling of the mold, which significantly affects porosity during formation. The highest thermal conductivity of the set (1.77 ± 0.05 W/(m·K)) was observed with 27 vol% magnesium oxide filling, which shows the effect of considerable structure porosity on the thermal conductivity of the composite material. Thereby, inevitable minimal porosity prevents a further rise in thermal conductivity on increase in the magnesium oxide filling content. Moreover, the important porosity decrease (by 20–25 %) in comparison with composite materials without hardening compound does not lead to a step-

wise increase in thermal conductivity. To clarify the mentioned above issue, the second set of the samples (5–8) was prepared with a different hardening compound content (from 5 to 25 wt% of the binder weight) and the same 25 % magnesium oxide volume filling.

A drastic decrease in the thermal conductivity of composite materials with 15 wt% hardening compound was observed (Fig. 3). This could be explained as follows: at a low sodium fluorosilicate content (5–10 wt%), it fully reacts with alkali in water glass with the formation of silica sol acid. The increase in the Na_2SiF_6 content leads to the accumulation of sodium fluorosilicate at the surface of magnesium oxide particles, which results in the decrease in thermal conductivity. The further increase in the content of curing agent content causes a decrease in porosity (from 20 to 14 %) and obviously an increase in thermal conductivity to 1.87 W/(m·K), which is explained based on the overall rise in the filling content owing to unreacted sodium fluorosilicate.
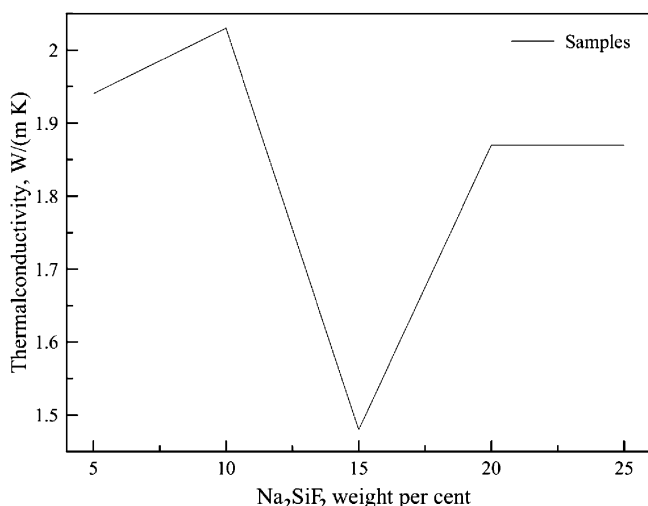

Fig. 3: Thermal conductivity of the third samples set with different Na_2SiF_6 content.

The residual sodium fluorosilicate content is confirmed by means of x-ray diffraction analysis (Fig. 4).
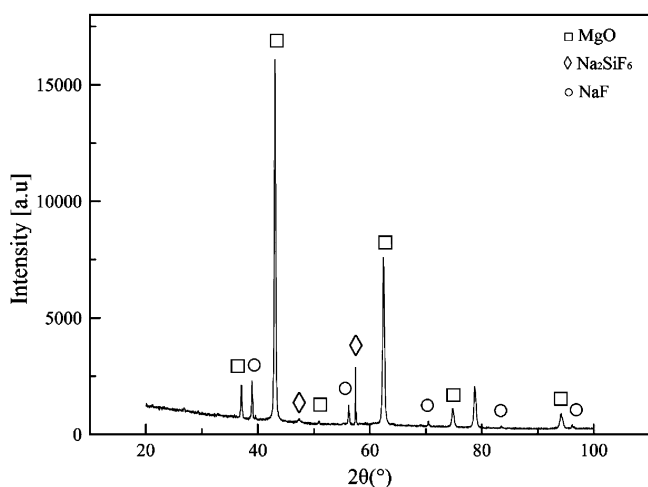

Fig. 4: X-ray diffraction analysis of water glass, magnesium oxide and sodium fluorosilicate mixture.

The third set of the samples (9–11) was used to study the influence of urea on the thermal conductivity and struc-

ture of composite materials. The compound for the third set of samples was a mixture of magnesium oxide, water glass, sodium fluorosilicate and urea (5–15 wt%). Physico-chemical processes as shown in the thermogram (Fig. 5) are similar to those of the previous set.
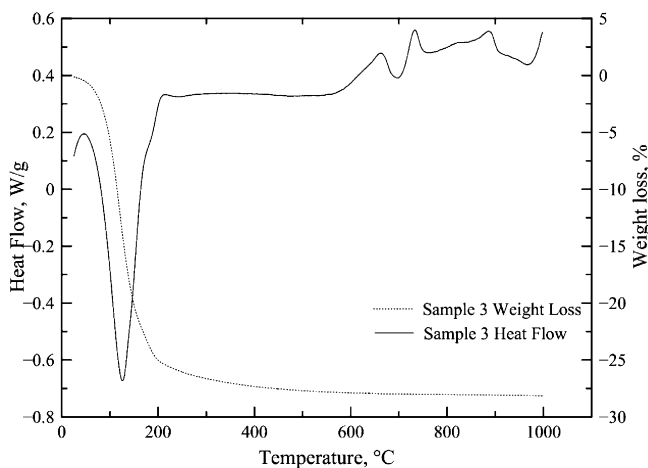

Fig. 5: Mixture of MgO, water glass, Na_2SiF_6 and urea.

Thermal conductivity decreases with increasing urea content, but it should be mentioned that measured data are still 24 % higher than those of samples without urea. On the basis of the experimental data, it is obvious that the optimal urea content is 5 wt%.

A change in the porosity of the samples was not observed, thus the considerable increase in thermal conductivity could only be explained based on phase content and/or material structure. According to x-ray diffraction analysis (Fig. 6), sodium fluoride and unreacted sodium fluorosilicate were not observed, at the same time sodium peroxide and sodium oxide were found. In light of the absence of a strong oxidizer, the emergence of sodium peroxide remains unclear.
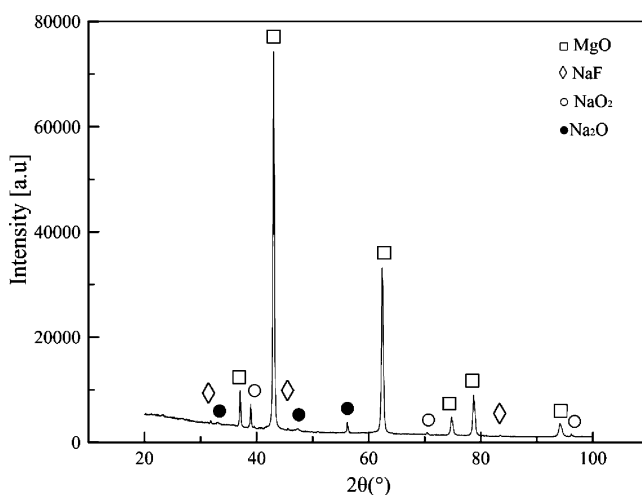

Fig. 6: X-ray diffraction analysis of composite material with urea addition.

Neither sodium oxide nor sodium peroxide has sufficient thermal conductivity; moreover paper [10] points out that an increase in the content of sodium oxide content leads to a decrease in thermal conductivity. It was suggested that the lack of sodium fluorosilicate, which has extremely

low thermal conductivity coefficient, at the magnesium oxide particle surface, results in an increase of the heat flow at the filler (magnesium oxide) and binder (water glass) boundary.

One special interest is the influence of graphite powder on the thermal characteristics of composite materials. It is generally known [13–15] that graphite is an anisotropic material and, as a result, its thermal conductivity varies in a wide range depending on the direction of heat flow. However, even the smallest graphite thermal conductivity value is more than 90 W/(m·K), which is four times higher than the thermal conductivity of magnesium oxide.

The fourth set of samples was prepared with an equal volume filling content and with a different C:MgO weight ratio. The following dependence was observed, that is that an increase in the C:MgO ratio effects a considerable decrease in thermal conductivity from 2.27 W/(m·K) to 1.53 W/(m·K). As the composite materials have an equal volume filling content and magnesium oxide and graphite have different densities, the weight filling content decreases, which clarifies such a dependence.

The lower the weight filling content and the lower the viscosity of samples during filling, the lower the porosity of a material was obtained after its formation. The highest volume filling achieved with pure graphite filler was 47 %, that is about two times more than the value for magnesium oxide (although the weight filling is equal this case). The sample has the highest thermal conductivity 3.71 W/(m·K). The cost of this composite material cost is equal to that of the silicone-based SPT-1 commonly used in different branches of industry. But the thermal conductivity of such a paste is less than 1.0 W/(m·K). According to the achieved results, the industrial application of the new pastes could be suggested.

The highest volume filling content with a mixed filler (C:MgO weight ratio 1:1) was 35 %, the thermal conductivity of such material is 3.09 W/(m·K).

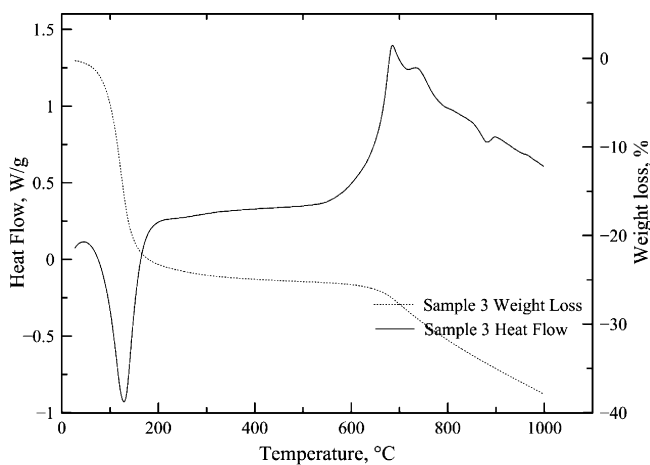The thermogram is shown in Fig. 7.

Fig. 7 : Thermogram of composite material with pure graphite filler.

At 683 °C, intensive burnout of the graphite is observed (70.55 J/g), and up to 1000 °C the additional composite material weight loss is 12.65 %. The exothermal reaction overrides other peaks, this resulted from xerogel formation as in previous samples. Only two peaks with a sufficient thermal effect are clearly observed, namely: crystal-

lization with the formation of complex silicates and sodium fluoride melting.

Based on the thermogram, graphite presents a prospective thermal conductive filler for composite material, however, the working temperatures of such material cannot be more than 500 °C in an air environment. Therefore calcination of samples for moisture evaporation was conducted in a nitrogen atmosphere to exclude graphite burnout.

IV. Conclusions

- As a result of moisture evaporating from the binder. 27 % weight loss has a considerable effect on the porosity of the samples. The average porosity of the composite materials is about 20 %;
- Owing to the addition of curing agent application, the total porosity of the samples has been reduced, the sodium fluorosilicate dependence on thermal conductivity has also been studied. Based on sophisticated hardening compound content – thermal conductivity relationship, the optimum quantity of sodium fluorosilicate is 10 wt%.
- According to thermal analysis, the application of urea as a stabilizer slightly affects the physicochemical processes in the chemistry and temperatures of the composite materials, however, phase composition differs significantly from the other samples, and owing to the absence of sodium fluorosilicate, a considerable increase in thermal conductivity is observed;
- The highest thermal conductivity of the composite material with urea addition is achieved at 5 wt% urea;
- Graphite powder as a filler has a considerable influence on thermal conductivity (3.71 W/(m·K)), mixed magnesium oxide-graphite (MgO:C 1:1 weight ratio) filler has a thermal conductivity coefficient of about 3.09 W/(m·K);
- Despite the high thermal conductivity of composite materials with a graphite filler, such materials could be applied at working temperatures below 500 °C in air environment or at a higher working temperatures in vacuum or inert atmospheres;
- Inorganic thermal conductive materials could be widely applied in LED and microelectronics.

References

1   Yung, K.C., Liem, H., Choy, H.S.: Heat dissipation performance of a high-brightness LED package assembly using high-thermal conductivity filler, *Appl. Optics*, **35**, [52], 8484 – 8493, (2013).

2   Anithambigai, P., Shanmugan, S., Mutharasu, D., Zahner, T., Lacey, D.: Study on thermal performance of high power LED employing aluminium filled epoxy composite as thermal interface material, *19th International Workshop on Thermal Investigations of ICS and Systems (Thermic)*, 181 – 187, (2013).

3   Shen, Q., Sun, D., Xu, Y., Jin, T., Zhao, X.: Orientation effects on natural convection heat dissipation of rectangular fin heat

sinks mounted on LEDs, *Int. J. Heat Mass Tran.*, **75**, 462 – 469, (2014).

4 Yu, J., Lacy Jr., T.E., Toghiani, H., Pittman Jr., C.U.: Micromechanically-based effective thermal conductivity estimates for polymer nanocomposites, *Compos. Part B-Eng.*, **53**, 267 – 273, (2013).

5 Wang, S., Qiu, J.: Enhancing thermal conductivity of glass fiber/polymer composites through carbon nanotubes incorporation, *Compos. Part B-Eng.*, **7**, [41], 533 – 536, (2010).

6 Harada, M., Hamaura, N., Ochi, M., Agari, Y.: Thermal conductivity of liquid crystalline epoxy/BN filler composites having ordered network structure, *Compos. Part B-Eng.*, **55**, 306 – 313, (2013).

7 Choi, S., Kim, J.: Thermal conductivity of epoxy composites with a binary-particle system of aluminum oxide and aluminum nitride fillers, *Compos. Part B-Eng.*, **51**, 140 – 147, (2013).

8 Gardea, F., Lagoudas, D.C.: Characterization of electrical and thermal properties of carbon nanotube/epoxy composites, *Compos. Part B-Eng.*, **56**, 611 – 620, (2014).

9 Ren, L., Pashayi, K., Fard, H.R., Kotha, S.P., Borca-Tasciuc, T., Ozisik, R.: Engineering the coefficient of thermal expansion and thermal conductivity of polymers filled with high aspect ratio silica nanofibers, *Compos. Part B-Eng.*, **58**, 228 – 234, (2014).

10 Shishkin, R.A., Erkhova, N.A., Beketov, A.R., Elagin, A.A.: Water-glass-based thermal paste for high temperature applications, *J. Ceram. Sci. Tech.*, **5**, 199 – 202, (2014).

11 Duderov, Y.G., Duderov, I.G.: Ceramic technology calculations: Handbook, Moscow, Stroyizdat, 80, (1973).

12 Iler, R.K.: The chemistry of silica: Solubility, polymerization, colloid and surface properties and biochemistry of silica, M. Mir, 892, (1982).

13 Park, J.M., Kwon, D.J., Wang, Z.J., Roh, J.U., Lee, W.I., Park, J.K., DeVries, K.L.: Effects of carbon nanotubes and carbon fiber reinforcements on thermal conductivity and ablation properties of carbon/phenolic composites, *Compos. Part B-Eng.*, **67**, 22 – 29, (2014).

14 Lachheb, M., Mustapha, K., Fethi, A., Sassi, B.N., Magali, F., Patrik, S.: Thermal properties measurement and heat storage analysis of paraffin/graphite composite phase change material. *Compos. Part B-Eng.*, **66**, 518 – 525, (2014).

15 Chen J.K., Huang I.S.: Thermal properties of aluminum-graphite composites by powder metallurgy. *Compos. Part B-Eng.*, **44**, 698 – 703, (2013).